




## Microbial repellence properties of engineered spider silk coatings prevent biofilm formation of opportunistic bacterial strains

Christoph Sommer, and Hendrik Bargel, Department of Biomaterials, University of Bayreuth, Bayreuth, Germany

Nadine Raßmann, Department of Physical Chemistry II, University of Bayreuth, Bayreuth, Germany

Thomas Scheibel , Department of Biomaterials, University of Bayreuth, Bayreuth, Germany; Bayreuth Center of Material Science and Engineering (BayMat), Bavarian Polymer Institute (BPI), Bayreuth Center of Colloids and Interfaces (BZKG), Bayreuth Center for Molecular Biosciences (BZMB), University of Bayreuth, Bayreuth, Germany

Address all correspondence to Thomas Scheibel at [thomas.scheibel@bm.uni-bayreuth.de](mailto:thomas.scheibel@bm.uni-bayreuth.de)

(Received 28 January 2021; accepted 30 March 2021; published online: 19 April 2021)

### Abstract

Bacterial infections are well recognised to be one of the most important current public health problems. Inhibiting adhesion of microbes on biomaterials is one approach for preventing inflammation. Coatings made of recombinant spider silk proteins based on the consensus sequence of *Araneus diadematus* dragline silk fibroin 4 have previously shown microbe-repellent properties. Concerning silicone implants, it has been further shown that spider silk coatings are effective in lowering the risk of capsular fibrosis. Here, microbial repellence tests using four opportunistic infection-related strains revealed additional insights into the microbe-repellent properties of spider silk-coated implants, exemplarily shown for silicone surfaces.

### Introduction

Multidrug resistant bacteria are recognised as one of the greatest threats to human health worldwide.<sup>[1]</sup> Further, rising rates of antibacterial resistance impact all aspects of modern medicine and threaten the effectiveness of many medical treatments in cancer care, transplantation and surgical procedures among others.<sup>[2]</sup>

*Staphylococcus aureus* is probably one of the most prevalent, dangerous and clinically relevant bacteria due to its methicillin resistance.<sup>[3,4]</sup> It is a leading cause of bacteremia and infective endocarditis and already spread beyond the confines of health-care facilities, emerging as a new threat in the community and becoming a dominant pathogen.<sup>[5,6]</sup>

Apart from *S. aureus*, other pathogens cause increasingly inflammatory problems. *Brevundimonas diminuta* found in infections of intravascular catheters are opportunistic pathogens affecting patients suffering from several diseases.<sup>[7,8]</sup> *Ralstonia* species are gram-negative bacilli that have increasingly been recognised as emerging nosocomial pathogens, particularly in immune-compromised hosts. *Ralstonia pickettii* is clinically the most important pathogen from the *Ralstonia* genus. Nosocomial outbreaks of *R. pickettii* infections are often based on contaminated medical solutions, including saline, sterile water, as well as disinfectants, and there have been case reports of various invasive infections<sup>[9,10]</sup> causing meningitis, infective endocarditis, nosocomial pneumonia, central line-associated bloodstream infection,<sup>[11]</sup> and chronic haemodialysis linked to contamination of the dialysis water.<sup>[12]</sup> *Propionibacterium acnes* is a microaerophilic, gram-positive and rod-shaped bacterium that resides in the pilosebaceous follicles of the human skin.<sup>[13]</sup> It is a low virulence opportunistic pathogen with the

potential to cause a wide range of infections, usually following surgery and often associated with the use of medical devices,<sup>[14]</sup> especially with breast implants.<sup>[15]</sup> Cases of elbow joint and prosthetic joint infections as well as post-operative discitis are reported.<sup>[16–18]</sup> *B. diminuta*, *R. pickettii*, *S. aureus* and *P. acnes* could also be found in bacterial inflammation incidences related to breast implant surgery and post-implant complications.<sup>[19–21]</sup> In fact, biofilm formation on the breast implant surface and the subsequent chronic inflammation are considered among the triggers of capsular contracture development<sup>[22]</sup> representing the most common complication following breast implant insertion and is the leading course for reoperation.<sup>[23]</sup>

To prevent biofilm formation, a material with initial microbial repellence properties would be beneficial to prevent overuse of antibiotics and, therefore, inhibit developing of multidrug-resistant microbes. This material could be used as a coating for established biomaterials such as silicone surfaces.<sup>[24,25]</sup>

Natural spider silk is microbe repellent, hypoallergenic, biocompatible and biodegradable, and possesses outstanding mechanical properties.<sup>[26,27]</sup> However, the application of natural spider silks in medical devices is limited due to their low accessibility, the lack of possible modifications and a high batch-to-batch variation common to most natural materials.<sup>[28]</sup>

The engineered silk protein eADF4(C16) is based on a major ampullate spidroin of the dragline silk of the European garden spider (*Araneus diadematus*). Additional data concerning the chemical structure is shown in Online Resource 1.<sup>[28,29]</sup> eADF4(C16) can be produced recombinantly at large scale as well as processed into a variety of morphologies other than fibres<sup>[30]</sup> such as films for coatings<sup>[27,31–35]</sup> or soft hydrogels for biofabrication.<sup>[36–38]</sup> In this context, it

has been shown to be a promising material for coating of polyurethane, polytetrafluoroethylene or silicone-based materials.<sup>[29]</sup>

Materials made of eADF4(C16) are perfectly suited for biomedical applications since they display the absence of toxicity, lack of immune reactivity and slow biodegradation.<sup>[39,40]</sup> Recently published results indicate that bacterial infestation of spider silk surfaces is inhibited by microbe-repellent properties of the material's surface rather than by antibacterial means.<sup>[41–44]</sup> As eADF4(C16) lacks cell binding motifs, like most so far identified spider silk proteins, eADF4(C16)-coated implants and catheters display significantly reduced adhesion and proliferation of any cells as compared to non-treated ones.<sup>[31,45]</sup> When transplanted into rats *in vivo*, eADF4(C16)-coated silicone implants exhibited a substantial reduction in capsular contracture. Interestingly, the four bacteria strains tested here are also sometimes associated with capsular contracture.<sup>[19,45]</sup>

In order to analyse the bacterial repellence properties of recombinant spider silk coatings against four selected inflammation-related bacteria, silicone surfaces with different surface topographies were used to further analyse its impact. *B. diminuta*, *R. pickettii*, *S. aureus* and *P. acnes* were incubated on the respective spider silk-coated silicone samples, and their repellence properties were evaluated accordingly.

## Materials and methods

### Surfaces and coating

Polydimethylsiloxane sheets of commercial materials with different texturing comprised POLYSmooth<sup>®</sup> (Smooth), MESMO<sup>®</sup> (Mesmo) and POLYtxt<sup>®</sup> (Polytxt) (POLYTECH, Germany) showing an average surface roughness of <1 µm for Smooth, 25 µm for Mesmo and 42 µm for Polytxt. Such materials are used as implant materials for breast implant surgery. They were washed with 80% ethanol and dried at room temperature overnight. Afterwards they were stored at room temperature for 4 weeks, placed on and covered with aluminium foil for further processing. Dip coating and fixation were performed in a clean bench (Hera guard, Eq ID 0011). The silicone squares were fixed with a tweezer and dipped for 10 s into isopropanol. After draining for 10–20 min, silicone squares were fixed with a tweezer and dipped for 5 min into eADF4(C16) coating solution at a concentration of 10 mg/mL. After draining the coating solution, the silicone squares were placed on a metal grit to dry for 2–3 h on the clean bench. Samples were dipped into 0.5 M sodium phosphate buffer (pH 7.4) for 30 s and washed with ultrapure (Milli-Q) water before 1 h of drying. An additional cleaning step was performed using isopropanol before the silicone squares were ready to use.

## Atomic force microscopy (AFM) measurements

The Smooth silicone samples were immobilised on microscopy slides as solid supports in order to prevent slipping during ongoing AFM measurements. Briefly, the microscopy slides were cleaned in a two-step procedure using alkaline Hellmanex cleaning solution (2% in ultrapure water) and a mixture of isopropanol (VWR) and water at a ratio of 3:1 (v:v). After drying, the glass was treated with air plasma for 10 min (Zepto, Diener Electronics). A thin film of Norland Optical Adhesive 63 (Norland Adhesives) was bladed onto the surface of the glass, and pieces of silicone samples (10 mm × 15 mm) were placed onto it. The glue was cured for 120 s under UV light.

The film thickness and swelling in PBS buffer (Sigma Aldrich, 1:10 diluted) were determined using AFM imaging in PeakForce Tapping Mode. All experiments were performed on a Dimension ICON (Bruker, Santa Barbara, CA) equipped with a Nanoscope V controller using SNL standard liquid imaging cantilevers (Bruker, Santa Barbara, CA) with a nominal spring constant of 0.35 N/m. Prior to the experiment, the spring constants of the cantilevers were calibrated using integrated functions of the used AFM software (NanoScope 9.10) following the thermal noise method.<sup>[46]</sup> Eventually, the sensitivity was calibrated in either media used for measuring, air or 1:10 diluted PBS buffer, respectively. All images were acquired at a PeakForce Tapping frequency of 1 kHz at lateral scan rates of 0.2 Hz and a peak force of 2 nN. The PeakForce amplitude was set to 150 nm in air and was increased to 300 nm in liquid to improve stability of the data acquisition. The same position on the same scratch was investigated in dried and swollen state. Optical microscopy control allowed to realign the scan area in liquid surrounding. Several consecutive scans at the crack in liquid were performed to verify that the equilibrium degree of swelling had been reached. A step height analysis was conducted using Nanoscope Analysis (version 1.80, Bruker Santa Barbara, CA) to determine the film thickness in dried and swollen state, which allowed to evaluate the swelling ratio.

## Contact angle measurement

Silicone surfaces of the type Smooth, Mesmo and Polytxt were coated with eADF4(C16) or tested uncoated with four aqueous liquids, namely, ultrapure water, 0.9% sodium chloride isotonic saline (Berlin-Chemie AG, Germany), betadine betaisodona solution (Mundipharma GmbH, Frankfurt a.M., Germany) twofold diluted in isotonic saline, which resulted in a final composition of 50 mg/mL povidone iodine, 0.45% sodium chloride and minor components like glycerol, nonoxynol 9, disodium hydroxide, anhydrous citric acid, sodium hydroxide and potassium iodate, and Adams solution with 100,000 U/L bacitracin, 2 g/L cefazolin and 160 mg/L gentamicin in isotonic saline. 10 µL of the test fluids were applied on the silicone surfaces and immediately imaged using a Canon EOS 700D camera with a macro objective. The contact angles between

the sample surfaces and the fluid drops were assessed using the *drop analysis* module of the Image J software (NIH, USA).

### Bacteria culture

*Brevundimonas diminuta* (DSM 1635) and *Ralstonia pickettii* (DSM 6297) were plated from cryostocks on plate count agar (PCA) plates and incubated for 2 days at 29°C. *Staphylococcus aureus* (DSM 799) was plated from cryostocks on PCA plates and incubated for 1 day at 37°C. *Propionibacterium acnes* (DSM 1897) was plated from cryostocks on Columbia blood agar plates and incubated for 7 days at 37°C at anaerobic conditions. Using an inoculating loop, bacteria were transferred from agar into 5 mL of 1/500 nutrient broth medium and evenly dispersed. The number of bacteria was determined using spectrophotometry (OD<sub>600</sub>), and the suspension was diluted 1/500 in nutrient broth to a final concentration of 5.0 × 10<sup>5</sup> cells/mL. The test inoculum was used within 2 h of preparation.

Bacterial solutions (1.25 × 10<sup>4</sup> CFU/cm<sup>2</sup> test area) were applied on the sample surfaces. To avoid drying out, samples were kept in a water-saturated environment for the 24 h cultivation period at 37°C. In order to remove the unbound cells, the surfaces were washed with sterile phosphate-buffered saline for 10 min with continuous shaking. Adhered cells were removed using ultrasound treatment and vortexing. Different dilutions of the washing solutions were incubated on culture plates, and colony numbers were determined.

### Scanning electron microscopy (SEM)

To analyse the morphological structure and bacterial infestation using SEM, the surfaces were fixed in paraformaldehyde solution (3.7% in 1× PBS buffer, Carl Roth GmbH, Germany) for 30 min, washed afterwards using 1× PBS buffer and dried for 2 days at 37°C. The samples were fixed on SEM stubs using conductive adhesive pads (12 mm, PLANO GmbH, Germany), sputter coated with 1.3 nm platinum (Sputter Coater EM ACE600, Leica, Germany) and imaged at 5 kV accelerating voltage using the SE2-Detector in Standard Mode using a FEG-SEM after oxygen plasma treatment for 1 min to minimise contaminations (Apreo VS, FEI/ThermoFisher Scientific, Germany).

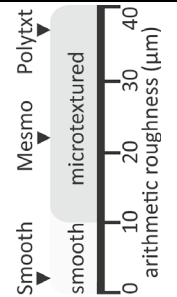
## Results and discussion

### Contact angle measurements

Surface hydrophobicity is important for a material's interaction with its environment; therefore, contact angles were analysed at the silicone-(coated/uncoated) air interface. Previous studies showed that bacterial growth on surfaces is inter alia traced back to hydrophilicity as bacteria need an optimised environment for growth and reproduction.<sup>[47]</sup> Table 1 shows contact angles of four different solutions typically used for handling and processing of breast implants. Ultrapure water, isotonic saline, betaisodona solution and Adams solution used as covering solutions ahead of implantation by surgeons. It needs to be stated that contact angles are influenced by the roughness of a surface according to Cassie and Baxter resulting in higher values than on smooth surfaces.<sup>[48]</sup> As the surface roughness of Mesmo and Polytxt silicone samples is 25 µm and 42 µm and the surface coating thickness is at the submicron level, the overall surface structure was not affected by the coating. Online Resource 2 shows SEM images of spider silk-coated and uncoated silicone surfaces at ×500 magnification indicating no topographical differences. All coated surfaces displayed a contact angle between 35° and 105°, and in some cases, significant differences were obtained concerning the hydrophilic properties in comparison to uncoated template surfaces (Smooth, Mesmo and Polytxt) with contact angles between 74° and 112°.

As described above, rougher surfaces had higher contact angles due to incomplete wetting of the material interface. This influenced significantly the results on textured surfaces,<sup>[48–50]</sup> but results of Smooth samples were significant. Apart from the water contact angle on Mesmo surfaces, all coated samples showed enhanced wetting with a contact angle reduction of up to 57% for betaisodona solution on Smooth samples, confirming water contact angle data in the literature.<sup>[34,51]</sup> Betaisodona solution and Adams solution showed the highest wettability of the tested solutions on spider silk coatings with 35°–75° (betaisodona) and 58°–88° (Adams), respectively. The highest hydrophilicity was detected for betaisodona solution on eADF4(C16) films with a contact angle of 35°.

**Table 1.** Surface hydrophilicity of uncoated and silk-coated silicone surfaces with different textures (Smooth, Mesmo and Polytxt) was determined using contact angle measurements.



Surface	Water	Isotonic saline	Betaisodona solution	Adams Solution	
Smooth	uncoated	99°±4°	99°±3°	81°±2°	74°±5°
	coated	56°±4°	65°±12°	35°±3°	58°±16°
Mesmo	uncoated	103°±5°	112°±5°	99°±4°	95°±5°
	coated	105°±5°	96°±7°	75°±17°	88°±9°
Polytxt	uncoated	106°±3°	107°±4°	80°±10°	81°±5°
	coated	93°±5°	71°±10°	71°±10°	81°±5°

Water, isotonic saline, betaisodona solution and Adams solution were dropped and analysed. *n* = 5.

### Coating thickness and swelling behaviour

Film thickness in dried state shown in Fig. 1(a) was determined from five PeakForce AFM images acquired on three different Smooth sample pieces. The average height was  $801 \text{ nm} \pm 185 \text{ nm}$ . For every image, the step height at the edge of the crack was determined across the whole image area in dry state [Fig. 1(c)] as well as in swollen state [Fig. 1(d)]. The roughness of the eADF4(C16) film and the silicone was evaluated to be  $20.4 \text{ nm}$  and  $16.1 \text{ nm}$  in an area of  $5 \mu\text{m} \times 5 \mu\text{m}$ , respectively.

In swollen state, a distinct increase in film thickness occurred to a height of approximately  $1.6 \mu\text{m}$  [Fig. 1(b)]. The swelling factor accounted to  $2.03 \pm 0.03$ . In addition to swelling in height, lateral swelling of the film was observed. No changes in film thickness were observed upon consecutive scans within the measurement time of 3 h. Thus, it can be concluded that the equilibrium swelling was reached before the beginning of the first scan at time scales  $< 30 \text{ min}$ .

### Bacterial repellence of spider silk-coated silicone surfaces

Biofilm formation of *B. diminuta*, *R. pickettii*, *S. aureus* and *P. acnes* was investigated on spider silk-coated as well as uncoated Smooth, Mesmo and Polytxt silicone surfaces. Microbial viability was quantified by plating the initial media and the washing buffers on media plates and counting cell colonies. Tables with raw data are shown in Online Resource 3. The reduction of cell numbers found on coated surfaces was normalised to uncoated surfaces for *B. diminuta* and *R. pickettii* and is shown in Fig. 2(a).

Bacterial repellence properties of the eADF4(C16)-coated silicone surfaces were predominant for *B. diminuta* and *R. pickettii*, which showed a reduction of adhesion between 79.4 and 99.7%, respectively. The negligible adhesion of *S. aureus* and *P. acnes* on the surfaces resulted in very low colony numbers, which prevented analysis of adhesion differences. In case of *P. acnes* incubated on coated and uncoated Polytxt surfaces, no difference in colony numbers could be observed after washing, as repellence properties were high regardless of the surface coating. The reduction of cell numbers found

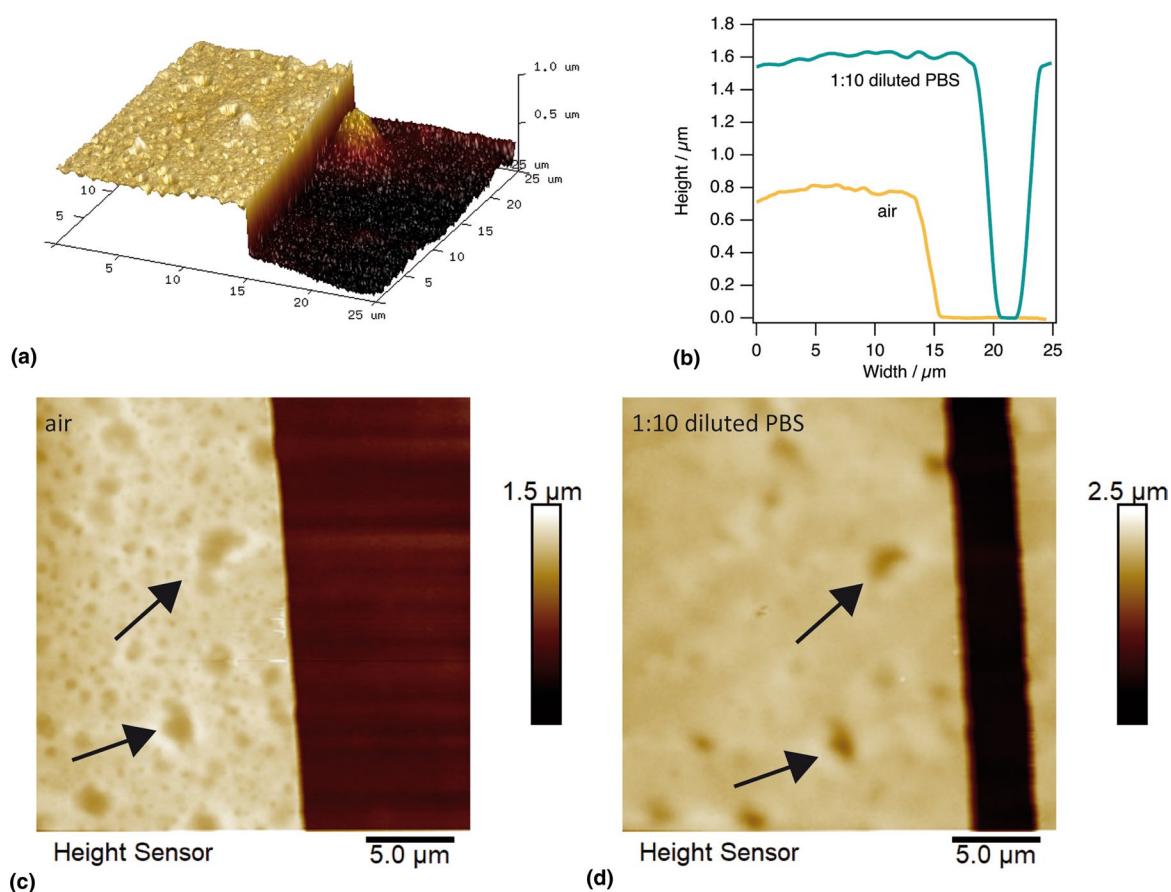
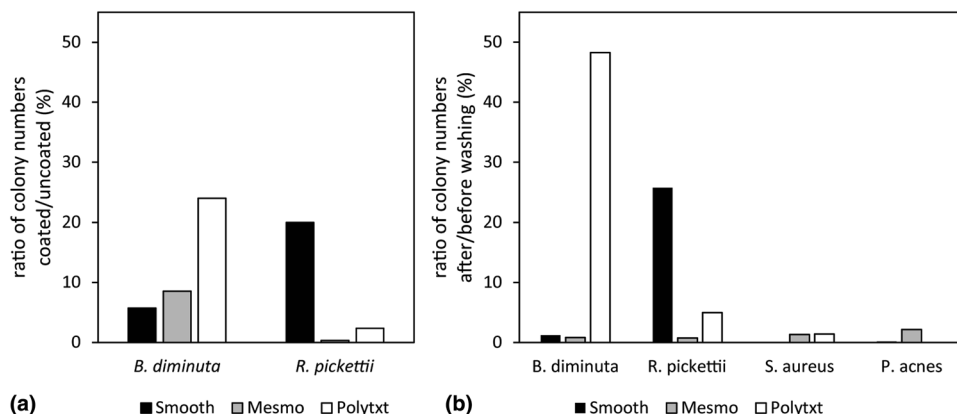


**Figure 1.** Results of AFM measurements on an eADF4(C16)-coated Smooth sample. (a) AFM Peak Force height measurements were captured at the edge of a crack on the eADF4(C16) coating. (b) Height of coating was measured in air and liquid (1:10 diluted PBS) environment, and height images were taken at the same edge position of a crack in (c) dried and (d) swollen state. Arrows indicate characteristic marks in the coating.

**Figure 2.** Results of adhesion tests using bacterial strains *B. diminuta*, *R. pickettii*, *S. aureus* and *P. acnes*. The ratio of colony numbers of spider silk-coated silicone sheets after washing are shown normalised to (a) colony numbers of uncoated silicone surfaces after washing and (b) to initial colony numbers on uncoated surfaces before incubation and washing. Ratio is given in %.



on coated surfaces normalised to cell numbers in the initial media for *B. diminuta* and *R. pickettii*, *S. aureus* and *P. acnes* is shown in Fig. 2(b). It could be concluded that *S. aureus* and *P. acnes* showed in general a low adhesion to the silicone surfaces; hence, a low ratio of adhered colonies after incubation to colony numbers could be detected in solution prior to incubation. Nevertheless, the spider silk coating promoted and improved repellence down to 0.01–1.41% for *P. acnes* and 0.01–2.17% for *S. aureus* [Fig. 2(b)]. It has been previously shown that surfaces of recombinant spider silk materials have bacterial repellence properties for other pathogens like *E. coli*, *S. mutans*, *P. pastoris* and *C. albicans*. In this previous study, *S. aureus* was also tested and showed a low adhesion force to the spider silk surfaces, which explains the resulting low colony numbers.<sup>[44]</sup>

Next, uncoated and coated silicone surfaces incubated with *B. diminuta*, *R. pickettii*, *S. aureus* and *P. acnes* (Fig. 3) were analysed using SEM, which confirmed that regardless of the silicone surface, the spider silk coating substantially restricted the attachment, growth and microbial colonisation. Uncoated textured surfaces like Polytxt and Mesmo showed slightly higher biofilm formation than Smooth ones due to a higher surface area.<sup>[52]</sup> In general, low adherence for *S. aureus* and *P. acnes* could be observed in both the absence and presence of the spider silk coatings [Fig. 3(c) and (d)].

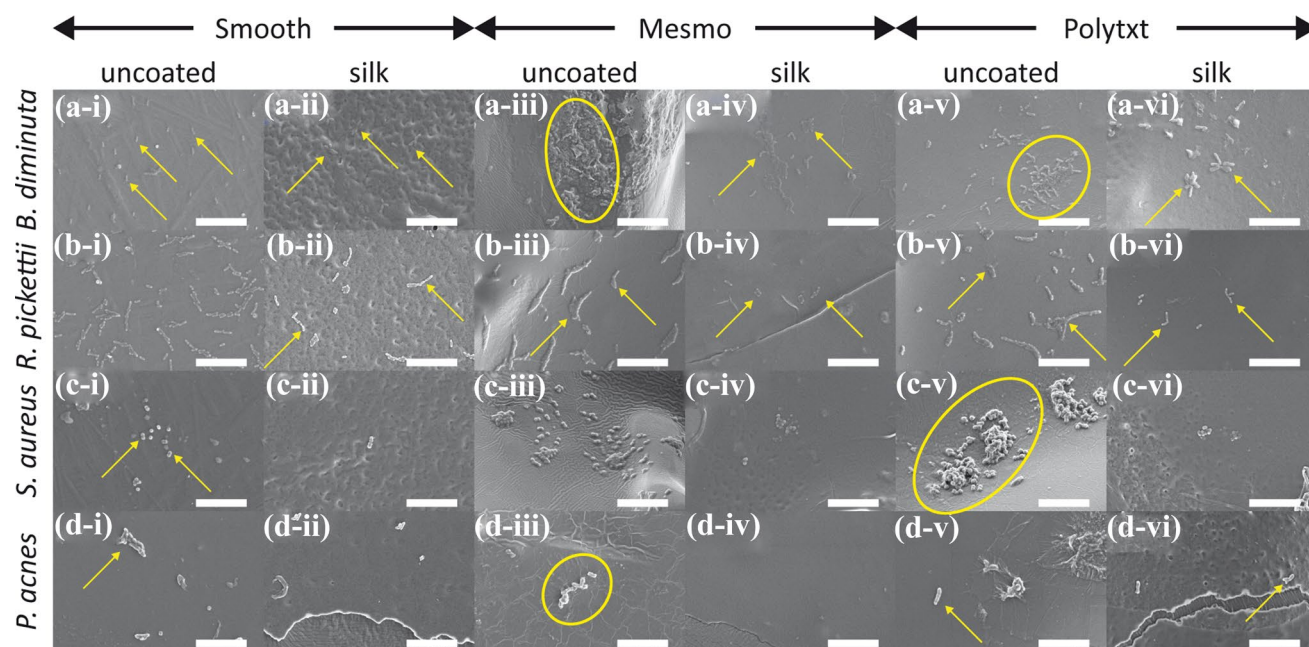


**Figure 3.** Bacterial repellence properties of silicone surfaces w/o coatings made of recombinant spider silk. SEM images showing (i, iii and v) uncoated and (ii, iv and vi) coated silicone surfaces after 24 h of incubation with (a) *B. diminuta*, (b) *R. pickettii*, (c) *S. aureus* and (d) *P. acnes* at 37°C on (i and ii) Smooth, (iii and iv) Mesmo and (v and vi) Polytxt materials. Arrows and circles indicate individual microbial cells or biofilms, respectively. Scale bars = 10 µm.

## Conclusion

Coatings of silicone surfaces made of recombinant spider silk eADF4(C16) improved wetting of such surfaces using different pre-surgical aseptic solutions, which in combination with spider silk's repellence properties enhances their applicability against opportunistic bacterial strains associated with inflammation. The repellence properties of spider silk coatings reduced microbial adherence up to 99.7% in comparison to uncoated silicone surfaces, and SEM images showed a significant decrease in biofilm formation after 24 h of incubation. Together with their biocompatibility and biodegradability, spider silk coatings could be part of a strategy to prevent inflammation and to reduce post-operative complications of implants.

## Acknowledgments

The author gratefully acknowledges POLYTECH Health & Aesthetics GmbH (Germany) for providing silicone implant materials. This work was supported by Dr. Brünke MTC e.K.—Microbiological Testing Competence (Germany) concerning bacterial repellence tests. We thank Prof. Dr. Papastavrou and Dr. Nicolas Helfricht and the Department of Physical Chemistry II for support concerning AFM measurements.

## Funding

Open Access funding enabled and organized by Projekt DEAL. No explicit funding was obtained for this study.

## Data availability

The supplementary material for this article can be found at <https://doi.org/10.1557/s43579-021-00034-y>.

## Declaration

### Conflict of interest

The authors declare the following competing financial interest: TS is co-founder and shareholder of AMSilk GmbH.

## Open Access

This article is licensed under a Creative Commons Attribution 4.0 International License, which permits use, sharing, adaptation, distribution and reproduction in any medium or format, as long as you give appropriate credit to the original author(s) and the source, provide a link to the Creative Commons licence, and indicate if changes were made. The images or other third party material in this article are included in the article's Creative Commons licence, unless indicated otherwise in a credit line to the material. If material is not included in the article's Creative Commons licence and your intended use is not permitted by statutory regulation or exceeds the permitted use, you will need to obtain permission directly from the copyright holder. To view a copy of this licence, visit <http://creativecommons.org/licenses/by/4.0/>.

## Supplementary Information

The online version contains supplementary material available at <https://doi.org/10.1557/s43579-021-00034-y>.

## References

1. B. Spellberg, M. Blaser, R.J. Guidos, H.W. Boucher, J.S. Bradley, B.I. Eisenstein, D. Gerding, R. Lynfield, L.B. Reller, J. Rex, D. Schwartz, E. Septimus, F.C. Tenover, D.N. Gilbert, Combating antimicrobial resistance: policy recommendations to save lives. *Clin Infect Dis* **52**, S397–428 (2011)
2. F. Perez, D. van Duin, Carbapenem-resistant Enterobacteriaceae: a menace to our most vulnerable patients. *Cleve Clin J Med* **80**, 225 (2013)
3. F.R. DeLeo, M. Otto, B.N. Kreiswirth, H.F. Chambers, Community-associated methicillin-resistant *Staphylococcus aureus*. *The Lancet* **375**, 1557 (2010)
4. W. Witte, Community-acquired methicillin-resistant *Staphylococcus aureus*: what do we need to know? *Clin Microbiol Infect* **15**, 17 (2009)
5. S. Deresinski, Methicillin-resistant *Staphylococcus aureus*: an evolutionary, epidemiologic, and therapeutic odyssey. *Clin Infect Dis* **40**, 562 (2005)
6. S.Y.C. Tong, J.S. Davis, E. Eichenberger, T.L. Holland, V.G. Fowler, *Staphylococcus aureus* infections: epidemiology, pathophysiology, clinical manifestations, and management. *Clin Microbiol Rev* **28**, 603 (2015)
7. X.Y. Han, R.A. Andrade, *Brevundimonas diminuta* infections and its resistance to fluoroquinolones. *J Antimicrob Chemother* **55**, 853 (2005)
8. M.P. Ryan, J.T. Pembroke, *Brevundimonas* spp: emerging global opportunistic pathogens. *Virulence* **9**, 480 (2018)
9. M.P. Ryan, J.T. Pembroke, C.C. Adley, *Ralstonia pickettii*: a persistent gram-negative nosocomial infectious organism. *J Hosp Infect* **62**, 278 (2006)
10. J. Orme, T. Rivera-Bonilla, A. Loli, N.N. Blattman, Native valve endocarditis due to *Ralstonia pickettii*: a case report and literature review. *Case Rep Infect Dis* **2015**, 324675 (2015)
11. N. Nasir, M.A. Sayeed, B. Jamil, *Ralstonia pickettii* Bacteremia: an emerging infection in a tertiary care hospital setting. *Cureus* **11**, e5084 (2019)
12. D. Tejera, G. Limongi, M. Bertullo, M. Cancela, Bacteriemia por *Ralstonia pickettii* en pacientes en hemodiálisis: reporte de dos casos. *Rev Bras Ter Intensiva* **28**, 195 (2016)
13. E.A. Grice, J.A. Segre, The skin microbiome. *Nat Rev Microbiol* **9**, 244 (2011)
14. A. Perry, P. Lambert, Propionibacterium acnes: infection beyond the skin. *Expert Rev Anti Infect Ther* **9**, 1149 (2011)
15. U.M. Rieger, J. Mesina, D.F. Kalbermatten, M. Haug, H.P. Frey, R. Pico, R. Frei, G. Pierer, N.J. Lüscher, A. Trampuz, Bacterial biofilms and capsular contracture in patients with breast implants. *Br J Surg* **100**, 768 (2013)
16. M. Jones, M.K. Kishore, D. Redfern, Propionibacterium acnes infection of the elbow. *J Shoulder Elbow Surg* **20**, e22–e25 (2011)
17. V. Zeller, A. Ghorbani, C. Strady, P. Leonard, P. Mamoudy, N. Desplaces, Propionibacterium acnes: an agent of prosthetic joint infection and colonization. *J Infect* **55**, 119 (2007)
18. A.E. Harris, C. Hennicke, K. Byers, W.C. Welch, Postoperative discitis due to Propionibacterium acnes: a case report and review of the literature. *Surg Neurol* **63**, 538–541 (2005)
19. D. Ajdic, Y. Zoghbi, D. Gerth, Z. J. Panthaki, S. Thaller, The relationship of bacterial biofilms and capsular contracture in breast implants. *Aesthet Surg J* **36**, 297 (2016)
20. J.B. Cohen, C. Carroll, M.M. Tenenbaum, T.M. Myckatyn, Breast implant-associated infections: the role of the national surgical quality improvement program and the local microbiome. *Plast Reconstr Surg* **136**, 921 (2015)
21. J.L. Del Pozo, N.V. Tran, P.M. Petty, C.H. Johnson, M.F. Walsh, U. Bite, R.P. Clay, J.N. Mandrekar, K.E. Piper, J.M. Steckelberg, R. Patel, Pilot study of association of bacteria on breast implants with capsular contracture. *J Clin Microbiol* **47**, 1333 (2009)
22. W.P. Adams, Capsular contracture: what is it? What causes it? How can it be prevented and managed? *Clin Plast Surg* **36**, 119–126 (2009)
23. S.M.W. Pool, R. Wolthuisen, C.M. Mouës-Vink, Silicone breast prostheses: a cohort study of complaints, complications, and explantations between 2003 and 2015. *J Plast Reconstr Aesthet Surg* **71**, 1563 (2018)

24. J.W. Costerton, P.S. Stewart, E.P. Greenberg, Bacterial biofilms: a common cause of persistent infections. *Science* **284**, 1318 (1999)
25. D. Campoccia, L. Montanaro, C.R. Arciola, A review of the clinical implications of anti-infective biomaterials and infection-resistant surfaces. *Biomaterials* **34**, 8018 (2013)
26. L. Römer, T. Scheibel, The elaborate structure of spider silk: structure and function of a natural high performance fiber. *Prion* **2**, 154 (2008)
27. K. Spiess, A. Lammel, T. Scheibel, Recombinant spider silk proteins for applications in biomaterials. *Macromol Biosci* **10**, 998 (2010)
28. T.B. Aigner, E. DeSimone, T. Scheibel, Biomedical applications of recombinant silk-based materials. *Adv Mater* **30**, e1704636 (2018)
29. T. Scheibel, Spider silks: recombinant synthesis, assembly, spinning, and engineering of synthetic proteins. *Microb Cell Fact* **3**, 14 (2004)
30. G. Lang, S. Jokisch, T. Scheibel, Air filter devices including nonwoven meshes of electrospun recombinant spider silk proteins. *J Vis Exp* **75**, e50492 (2013)
31. C.B. Borkner, S. Wohlrab, E. Möller, G. Lang, T. Scheibel, Surface modification of polymeric biomaterials using recombinant spider silk proteins. *ACS Biomater. Sci. Eng.* **3**, 767 (2017)
32. U. Slotta, M. Tammer, F. Kremer, P. Koelsch, T. Scheibel, Structural analysis of spider silk films. *Supramol. Chem.* **18**, 465 (2006)
33. E. Metwalli, U. Slotta, C. Darko, S.V. Roth, T. Scheibel, C.M. Papadakis, Structural changes of thin films from recombinant spider silk proteins upon post-treatment. *Appl. Phys. A* **89**, 655 (2007)
34. S. Wohlrab, K. Spieß, T. Scheibel, Varying surface hydrophobicities of coatings made of recombinant spider silk proteins. *J. Mater. Chem.* **22**, 22050 (2012)
35. L. Eisoldt, A. Smith, T. Scheibel, Decoding the secrets of spider silk. *Mater. Today* **14**, 80 (2011)
36. S. Kumari, H. Bargel, M.U. Anby, D. Lafargue, T. Scheibel, Recombinant spider silk hydrogels for sustained release of biologicals. *ACS Biomater. Sci. Eng.* **4**, 1750–1759 (2018)
37. E. DeSimone, K. Schacht, A. Pellert, T. Scheibel, Recombinant spider silk-based bioinks. *Biofabrication* **9**, 44104 (2017)
38. C. Thamm, E. DeSimone, T. Scheibel, Characterization of hydrogels made of a novel spider silk protein eMaSp1s and evaluation for 3D printing. *Macromol. Biosci.* **17**, 1700141 (2017)
39. A. Leal-Egaña, G. Lang, C. Mauerer, J. Wickinghoff, M. Weber, S. Geimer, T. Scheibel, Interactions of fibroblasts with different morphologies made of an engineered spider silk protein. *Adv. Eng. Mater.* **14**, B67–B75 (2012)
40. S. Müller-Herrmann, T. Scheibel, Enzymatic degradation of films, particles, and nonwoven meshes made of a recombinant spider silk protein. *ACS Biomater. Sci. Eng.* **1**, 247 (2015)
41. R.H. Zha, P. Delparastan, T.D. Fink, J. Bauer, T. Scheibel, P.B. Messersmith, Universal nanothin silk coatings via controlled spidroin self-assembly. *Biomater Sci* **7**, 683 (2019)
42. S. Zhang, D. Piorkowski, W.-R. Lin, Y.-R. Lee, C.-P. Liao, P.-H. Wang, and I.-M. Tso: *Nitrogen inaccessibility protects spider silk from bacterial growth*. *J Exp Biol*, **222**(Pt 20) (2019).
43. A. Leal-Egaña, T. Scheibel, Silk-based materials for biomedical applications. *Biotechnol Appl Biochem* **55**, 155 (2010)
44. S. Kumari, G. Lang, E. DeSimone, C. Spengler, V.T. Trossmann, S. Lücker, M. Hudel, K. Jacobs, N. Krämer, T. Scheibel, Engineered spider silk-based 2D and 3D materials prevent microbial infestation. *Mater. Today* **41**, 21–33 (2020)
45. P.H. Zepelin, N.C. Maksimovikj, M.C. Jordan, J. Nickel, G. Lang, A.H. Leimer, L. Römer, T. Scheibel, Spider silk coatings as a bioshield to reduce periprosthetic fibrous capsule formation. *Adv. Funct. Mater.* **24**, 2658 (2014)
46. J.L. Hutter, J. Bechhoefer, Calibration of atomic-force microscope tips. *Rev. Sci. Instrum.* **64**, 1868 (1993)
47. X. Zhang, L. Wang, E. Levänen, Superhydrophobic surfaces for the reduction of bacterial adhesion. *RSC Adv.* **3**, 12003 (2013)
48. A.B.D. Cassie, S. Baxter, Wettability of porous surfaces. *Trans. Faraday Soc.* **40**, 546 (1944)
49. S. Barr, E.W. Hill, A. Bayat, Functional biocompatibility testing of silicone breast implants and a novel classification system based on surface roughness. *J Mech Behav Biomed Mater* **75**, 75 (2017)
50. A.A. Valencia-Lazcano, T. Alonso-Rasgado, A. Bayat, Characterisation of breast implant surfaces and correlation with fibroblast adhesion. *J Mech Behav Biomed Mater* **21**, 133 (2013)
51. J. Petzold, T.B. Aigner, F. Touska, K. Zimmermann, T. Scheibel, F.B. Engel, Surface features of recombinant spider silk protein eADF4(k16)-made materials are well-suited for cardiac tissue engineering. *Adv. Funct. Mater.* **27**, 1701427 (2017)
52. G.A. James, L. Boegli, J. Hancock, L. Bowersock, A. Parker, B.M. Kinney, Bacterial adhesion and biofilm formation on textured breast implant shell materials. *Aesthetic Plast Surg* **43**, 490 (2019)